

# The Three-Dimensional Distribution of Galactic AGB Stars with ALLWISE

Nicholas M. Hunt-Walker, Željko Ivezić, Andrew C. Becker

*University of Washington, Department of Astronomy, Seattle, WA 98195*

`nmhw@uw.edu, ivezic@uw.edu, acbecker@uw.edu`

## 1. Introduction

The structure of the Milky Way holds clues to the processes of formation and evolution of galaxies. Historical models typically assumed three discrete components described by simple analytic expressions: the thin disk, thick disk, and halo (Bahcall & Soneira 1980; Gilmore et al. 1989; Majewski 1993). Recent surveys, such as the Sloan Digital Sky Survey (SDSS, York et al. 2000) and the Two Micron All Sky Survey (2MASS, Skrutskie et al. 2006), have provided much more detail about these components. For example, SDSS data have constrained stellar distributions in the 7-dimensional space spanned by spatial coordinates (Jurić et al. 2008), velocity components (Bond et al. 2010), and metallicity (Ivezić et al. 2008). The resulting maps revealed rich, complex substructure in the distribution of the Milky Way’s stars (e.g. Ivezić et al. 2000; Yanny et al. 2000; Vivas et al. 2001; Newberg et al. 2002; Majewski et al. 2003; Belokurov et al. 2006; Grillmair 2006; Vivas & Zinn 2006), deeply shaking the older view of a smooth Galaxy.

The large distance limit of about 100 kpc for some halo populations (e.g. RR Lyrae and BHB stars with SDSS, Sesar et al. 2010 and red giants with 2MASS, Majewski et al. 2003), as well as about 10 kpc for very numerous main sequence stars, is not reached when studying disk component at low galactic latitudes. As shown, for example, by Berry et al. (2012), the extinction due to interstellar dust limits the SDSS sample of main sequence stars to heliocentric distances of only a few kpc. In order to avoid detrimental effect of dust extinction, stellar samples need to be probed at longer infrared wavelengths. Several infrared surveys covering the Galactic plane have recently become available (WISE, Wright et al. 2010; Cutri et al. 2012, GLIMPSE Churchwell et al. 2009; Benjamin et al. 2003, VVV Saito et al. 2012).

Among populations suitable for studying Galactic structure using infrared surveys, Asymptotic Giant Branch (AGB) stars stand out. AGB stars represent the last stage of evolution for stars between 0.8 and 8  $M_{\odot}$  (Iben & Renzini 1983; Herwig 2005). Stars from this mass range can reach the final stages of stellar evolution within the Galactic timescale ( $\sim 10$  Gyr, Iben & Renzini 1983) and thus are bound to reside throughout the Galaxy wherever other stars are present. This phase of stellar evolution is marked by two distinct episodes with different observational characteristics: the early AGB phase (E-AGB) and the thermally-pulsing AGB phase (TP). During the thermally-pulsing phase, AGB stars produce substantial dust-driven stellar winds ( $10^{-7} < \dot{M} < 10^{-4} M_{\odot} \text{ yr}^{-1}$ , Olofsson et al. 2002) rich in oxides (SiO, Al<sub>2</sub>O<sub>3</sub>, etc.) or carbon-rich molecules (SiC, amC, etc.). The dominant chemical composition is highly dependent upon the metallicity of the host

galaxy (Matsuura et al. 2005). High-metallicity galaxies like the Milky Way have a substantial population of oxygen-rich AGB stars (Habing et al. 1985), whereas low-metallicity galaxies such as the Magellanic clouds are dominated by carbon-rich AGB stars (Boyer et al. 2011). In both cases, the other species of AGB star is rarely seen, as richness in one chemical type (e.g. oxides) necessitates the almost complete capture of the other chemical type (e.g. carbon) in CO (Iben & Renzini 1983).

The dust-rich winds in TP phase create vast circumstellar shells that are warmed by the stellar photosphere and emit copiously in the near- and mid-infrared (NIR & MIR, respectively). Together with high bolometric luminosity ( $10^3$ – $10^4 M_\odot$ , Knauer et al. 2001), this redistribution of the output radiation to the infrared wavelength makes AGB stars excellent disk probe when infrared survey data are available. Indeed, they were detected all the way to the Galactic center even with the IRAS survey (Jackson et al. 2002). Such disk studies can now be significantly improved thanks to the much more sensitive WISE survey.

The *Wide-field Infrared Survey Explorer*, WISE, is a space observatory that has imaged essentially the entire sky in the MIR (3.4, 4.6, 12, and 22  $\mu\text{m}$ ). The WISE catalog has been positionally matched to the 2MASS catalog, with the matched catalog listing NIR and MIR 7-band photometry for hundreds of millions of sources. Given the depths of the two surveys, this catalog should contain AGB stars to many kpc beyond the Galactic center. Here we develop selection methods for AGB stars using WISE and 2MASS data, and analyse the resulting samples.

In Section 2, we describe in detail the WISE, 2MASS and other auxiliary data used in our study and the data reduction process. In Section 3, we use samples of known Galactic and Magellanic AGB stars to derive WISE-2MASS color-based selection criteria, and calibrate color-absolute magnitude relations. In Section 4, we describe the spatial density distribution of selected AGB candidates from the Milky Way. Our conclusions are summarized in Section 5.

## 2. Input Catalogs and Data Preparation

Our principal data source is the merged WISE-2MASS catalog. In order to derive WISE-2MASS color-based selection criteria, we use a homogenous sample of AGB stars from the OGLE-III Catalog of Variable Stars supplying objects in the Magellanic Clouds. This sample serves to calibrate color-color and color-absolute magnitude relations that underlie our distance estimates. In order to assess what infrared populations could contribute to contamination of selected AGB candidates, we utilize extragalactic sources from SDSS data release 7 pulled from the NYU Value-added Galaxy Catalog, the SDSS unofficial Luminous Red Galaxy sample, and young stellar objects identified in WISE data, also described below. We conclude this section by describing how these auxiliary catalogs were positionally merged with the WISE-2MASS catalog, summarize the object counts before and after quality control (Table 1), and summarize the effects of WISE-2MASS color-color cuts (Table 2) on the AGB and contaminant samples.

## 2.1. WISE-2MASS catalog

In this study, we rely heavily on data from the ALLWISE extension of the WISE survey, combining data from the initial All-Sky Data Release, the 3-band cryogenic data release, and the NEOWISE post-cryogenic data release (Cutri et al. 2013). The initial WISE All-Sky Data Release observed the sky between January and August 2010, observing the sky 1.2 times on average with four detectors, operating at 3.4, 4.6, 12, and 22  $\mu\text{m}$ . Hereon we refer to ALLWISE photometric bands at [3.4  $\mu\text{m}$ /4.6  $\mu\text{m}$ /12  $\mu\text{m}$ /22  $\mu\text{m}$ ] as [W1/W2/W3/W4]. The positions of objects in the WISE catalog were calibrated using the 2MASS point source catalog.

The 3-band cryogenic data release contains data from W1, 2, and 3, and surveyed 30% of the sky between August and October 2010. During the 3-band cryogenic survey, W1 and W2 operated with nearly the same sensitivity as during the full survey. Warming of the telescope reduced sensitivity in W3 and fully saturated W4. The NEOWISE post-cryogenic data release contains W1 and W2 measurements, with sensitivities close to those obtained during the full cryogenic phase. During this phase, WISE surveyed 70% of the sky. Data products from the post-cryogenic release included updated instrumental, astrometric, and photometric calibrations and reduction algorithms, resulting in higher signal-to-noise for most sources. The overall number of sources compiled into ALLWISE totals over 747.6 million.

## 2.2. AGB stars from the OGLE-III Catalog of Variable Stars

The OGLE-III Catalog of Variable Stars (CVS) (Udalski et al. 2008; Soszyński et al. 2009, 2011) is a subset of the overall OGLE-III dataset, containing roughly 10 years of observations in the *V*- and *I*-bands of over 120,000 variable stars, with typically 700-900 data points per star in the *I*-band and about 50 data points per star in *V*-band. With high-precision photometry ( $\sim 0.01$  mag, Soszynski et al. 2007), these observations saturate at  $I = 12.5$  mag, and are limited at the faint end at  $I = 20.5$  mag (Zebrun et al. 2001). The variability of these stars covers a wide range of periodicity ( $4 < P < 2000$  days) and amplitudes ( $0.005 < A_I < 5.7$  mag).

The OGLE-III CVS is accessible through an online database<sup>1</sup>, with long-period variables (LPVs) classified by object type, evolutionary status, and spectral type. Object type is based chiefly on variability and luminosity. OGLE Small Amplitude Red Giants (hereon OSARGs) are weakly-variable ( $0.005 < A_I < 0.13$  mag), with relatively short periods ( $10 < P < 100$  days; Soszynski et al. 2004). Additionally, because these objects are multiperiodic, OSARGs are selected using their period ratios and their distances from established period-luminosity ( $\log P - L$ ) sequences from Wood et al. (1999). For a more detailed description of their selection, see Soszynski et al. (2007). Mira variables and Semi-Regular Variables (hereon SRVs) are identified using *I*-band

---

<sup>1</sup><http://ogledb.astrouw.edu.pl/~ogle/CVS/>

amplitudes and  $P - W_I$ , where  $W_I$  is the reddening-free Wesenheit index (Soszynski et al. 2005):

$$W_I = I - 1.55(V - I) \quad (1)$$

As red giant branch stars (RGBs) can contaminate the same  $\log(P) - L$  space as AGB stars, evolutionary type is distinguished in two ways. Stars above the tip of the RGB ( $K_s = 12.05$  mag in LMC; Soszynski et al. 2004, 2007) are classified as AGBs. Below that threshold, a narrow sequence of stars appears to share the same slope and intercept with AGB stars above the TRGB. Additionally they share similar primary-secondary period ratios as known AGB stars (Soszynski et al. 2005). However, as there is still some contamination by RGBs using period ratios, we reject all OGLE objects below the TRGB.

For individual  $\log(P) - L$  sequences, spectral type (O-rich or C-rich) is easily seen as separations in  $\log(P) - L$  space as well as visible-NIR color-color space. The initial classifications are based on spectroscopically-observed stars and were extended more generally to  $\log(P) - L$  and visible-NIR color-color criteria (Soszynski et al. 2005, 2007). This clear separation can be seen in Figure 1.

From the initial OGLE-III sample of 52,976 LPVs, we retain 43,262 after matching to ALLWISE within  $3''$ , and ensuring only 1 match to 2MASS as well as all objects needing to be in the LMC. The  $I$ -band median of OGLE-III LPVs is  $\approx 14.68$  mag with a standard deviation of 0.72 mag. Out of the entire sample only 13 objects (Miras) fall beyond the 20.5 mag  $5\sigma$  faint limit, and 41 beyond the saturation limit. As such, we expect this to effectively represent the complete sample of oscillating AGB stars in the LMC.

Out of the 43,262 objects matched to ALLWISE within  $3''$ , 1,633 are Mira variables, 30,768 are OSARGs, and 10,861 are SRVs. The right side of Figure 1 shows color-color plots for OGLE-2MASS colors, with a line at  $(J - K_s) = 1.4$  drawn to separate O-rich and C-rich Miras. Out of the total of 457 O-rich Miras, 36 (7.9%) have  $(J - K_s) > 1.4$ . Conversely, out of the 1,176 C-rich total Miras, 1,138 (96.8%) have  $(J - K_s) > 1.4$ . The distribution of these objects on the sky is summarized in Figure 2.

### 2.3. Extragalactic catalogs from SDSS

SDSS is a multi-year survey of roughly 25% of the sky that collected both photometric ( $u$ ,  $g$ ,  $r$ ,  $i$ ,  $z$ -bands for 700+ million objects) and spectroscopic measurements (1.6+ million) of stars and extragalactic sources (York et al. 2000). Though its ground-based nature and sensitivity to interstellar extinction prevent SDSS from being an all-sky survey, it represents the largest spectrophotometric catalog to date. For this study we collect extragalactic objects from the NYU Value-added Galaxy Catalog, containing objects matched between SDSS and several auxiliary surveys spanning multiple wavelength regimes, and the SDSS Luminous Red Galaxy sample, isolating

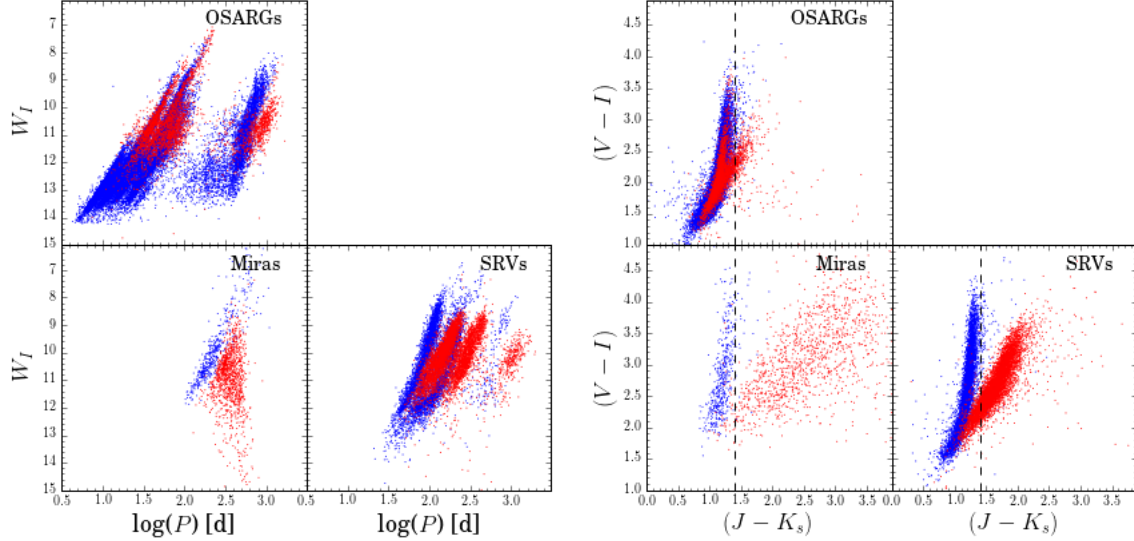


Fig. 1.— O-rich (*blue*) and C-rich (*red*) OGLE-III LPVs matched to 2MASS. *Left*:  $W_I$  vs log period in days. *Right*: OGLE-III  $(V-I)$  vs 2MASS  $(J-K_s)$ . The dashed line represents  $(J-K_s) = 1.4$ .

high-confidence luminous red galaxies from the SDSS database. The color-color distributions of these sample sets are shown in Figure 3.

### 2.3.1. The NYU Value-added Galaxy Catalog

In order to cull the full set of SDSS spectrophotometry and produce an easily-referenced extragalactic catalog for investigating galaxy formation and evolution, the NYU Value-added Galaxy Catalog (NYU-VAGC; Blanton et al. 2005) was created as of SDSS data-release 7 (DR7).

The NYU-VAGC contains matches between SDSS spectrophotometry and the following catalogs: the FIRST radio survey, the 2MASS Point Source Catalog, the 2MASS Extended Source Catalog, the Two-degree Field Galaxy Redshift Survey, the IRAS Point Source Catalog Redshift Survey, and Reference Catalog 3 (RC3.9b). As a consequence, the NYU-VAGC retains SDSS optical photometry in addition to spectral classifications (QSO, galaxy, star) and subclassifications (AGN, starforming galaxy, starburst galaxy, etc.) for 441,707 objects across 10,417 square degrees of the SDSS footprint. Main and secondary classifications are made by comparing measured optical spectra to the SDSS spectral library. See Blanton et al. (2005) for the full set of reduction and inclusion criteria. This catalog is available via an online data repository<sup>2</sup>, along with a full

<sup>2</sup><http://sdss.physics.nyu.edu/vagc/>

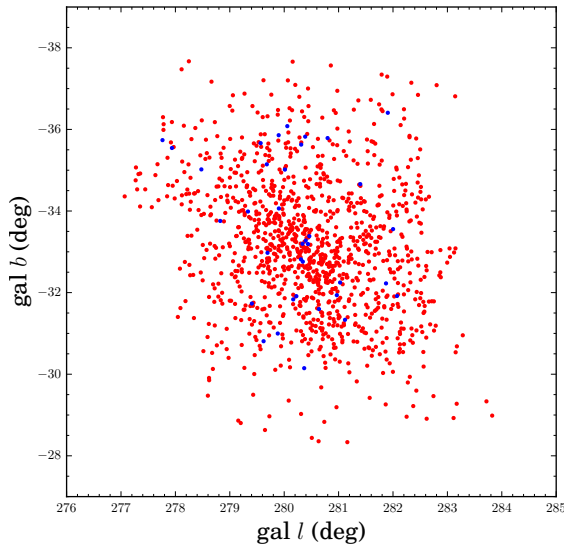


Fig. 2.— O-rich (*blue*) and C-rich (*red*) OGLE-III Miras with  $(J - K_s) > 1.4$ .

description of the data and other subsamples not used in this study. The populations for each species (QSO, AGN, starforming galaxy (SF), starburst galaxy (SB)) are found in Table 1.

### 2.3.2. The Luminous Red Galaxy Sample

Subselected for the study of Baryon Acoustic Oscillations by Kazin et al. (2010), the Luminous Red Galaxy sample (LRGs; Eisenstein et al. 2001) is also sourced from SDSS DR7. LRGs contaminate the IR color-color space of AGB stars due to their large redshifts ( $z \sim 0.3$ ). We obtain the LRG sample from the data repository<sup>3</sup> of Kazin et al. (2010). The initial sample is volume-limited, containing 105,631 objects spanning a redshift range of  $0.16 < z < 0.47$ .

## 2.4. WISE+2MASS Young Stellar Objects

Young Stellar Objects (YSOs) represent a unique contaminant in our search for dust-enshrouded AGB stars. Similar to AGBs, YSOs are luminous sources surrounded by warm, dusty environments. That warm dust can then glow brightly in the MIR, easily contaminating AGB color-color space. To characterize and later eliminate this potential contaminant, we select as our base sample 290 YSOs from Rebull et al. (2011), a survey searching for YSOs in the Taurus Molecular Cloud using data from WISE, ancillary data from SDSS and 2MASS, and covering 260 deg<sup>2</sup>. As YSO tend

---

<sup>3</sup><http://cosmo.nyu.edu/~eak306/SDSS-LRG.html>

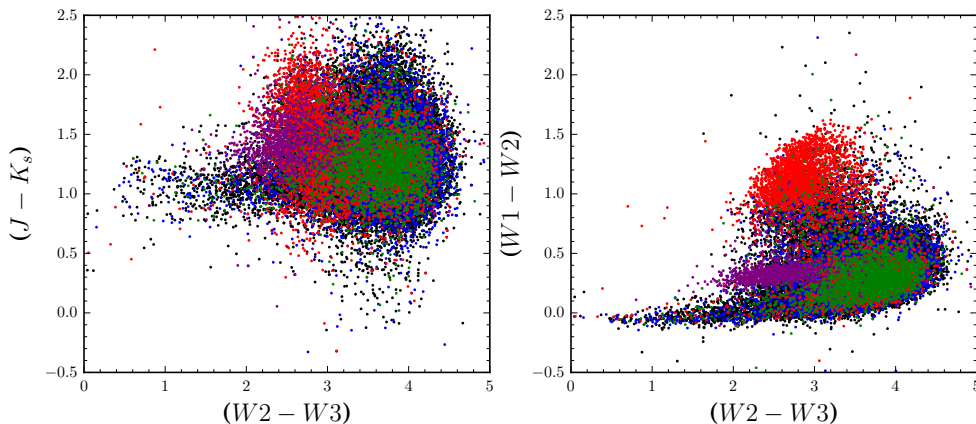


Fig. 3.— Extragalactic sources from SDSS DR7’s VAGC and LRG samples. Objects are (*black*) starforming galaxies, (*blue*) starburst galaxies, (*red*) QSOs, (*green*) AGN, and (*purple*) LRGs.

to be embedded within high-extinction clouds, we expect that the dust-reddened NIR/MIR emission from these objects should match to similar objects in the LMC when we later calibrate our color-color criteria.

## 2.5. WISE+2MASS Stellar Locus

The color-color space occupied by AGB stars showing significant photospheric emission is heavily populated by naked stars from the main sequence. By sheer number, these stars would drown out sources that could be AGB stars with thin circumstellar envelopes. To address this, we extract the stellar locus from ALLWISE in the direction of the LMC ( $276.5^\circ < l < 284^\circ$ ,  $-38.2^\circ < b < -28^\circ$ ). We require that every object have 1 2MASS association,  $[W1/W2/W3]$  signal-to-noise  $> 1$ , detections in 2MASS J, H, and K, and confusion & contamination flags set to 0 for  $[W1/W2/W3]$ . We then adapt the color-color criteria from [Davenport et al. \(2014\)](#). Their locus focuses on stars with effective temperatures  $3540 < T_{\text{eff}} < 7200K$ . We fit their criteria for  $J - K_s$  vs  $W1 - W2$  within  $3\sigma$  of the locus with degree-3 polynomials. The resulting fit for the  $3\sigma$  stellar locus follows:

$$(J - K_s) < 61.67(W1 - W2)^3 - 17.88(W1 - W2)^2 + 1.68(W1 - W2) + 0.99 \quad (2)$$

$$(J - K_s) > 40.19(W1 - W2)^3 - 9.78(W1 - W2)^2 + 0.54(W1 - W2) + 0.64 \quad (3)$$

The resulting locus sample, as well as the original [Davenport et al. \(2014\)](#) bounds and locus are shown in in Fig 4. Note that our sample goes beyond the limits of the stated locus.



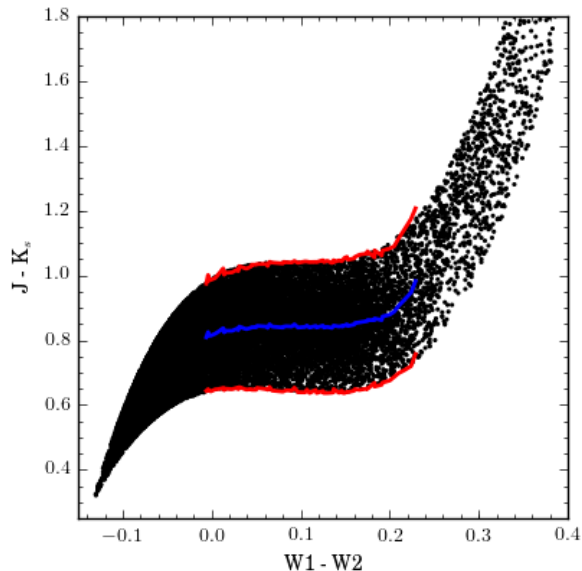


Fig. 4.— The WISE-2MASS stellar locus. (*black dots*) objects from the stellar locus in the direction of the LMC. (*blue line*) WISE-2MASS color-color stellar locus derived from [Davenport et al. \(2014\)](#). (*red line*)  $3\sigma$  boundaries for WISE-2MASS color-color locus.

## 2.6. Merged Samples

The OGLE-III AGB sample, as well as the SDSS and YSO samples, were matched to the ALLWISE data products via the GATOR tool at the NASA/IPAC Infrared Science Archive<sup>4</sup>. The accepted matching radius was 3'' except in the case of YSOs, which were limited to 1''. YSO objects were obtained from the VIZIER service already possessing WISE observations, so we were able to accept a smaller matching radius as we only sought the extra 2MASS information.

The final OGLE-2MASS-WISE AGB sample is produced from the object sample in section 2.2. We apply the point source saturation limits of  $[W1/W2/W3/K_s] < [2.0/1.5/-3.0/8.5]$ . We also enforce, in order, the  $5\sigma$  faint limits for  $[W1/W2/W3/K_s] < [16.83/15.6/11.32/15.5]$ . The WISE point source saturation and  $5\sigma$  faint limits can be found in [Cutri et al. \(2012\)](#). The 2MASS faint and saturation limits are found in [Skrutskie et al. \(2006\)](#). To ensure quality measurements in the desired bands, we also enforce  $[W1/W2/W3]$  SNR  $> 3$ , and contamination & confusion flags (`cc_flag`) set to 0 in each of those bands. The VAGC, LRG, and YSO samples are filtered through the same criteria. Note that we deliberately neglect  $W4$  because, after applying the  $5\sigma$  faint limits as well as `cc_flag`=0, our sample is too heavily reduced. For similar reasons, we only apply the `cc_flag` criteria to  $[W1/W2]$ , noting that clean flags in these two bands should be sufficient for source detection considering the extended NEOWISE mission contains extra observations for these

<sup>4</sup><http://irsa.ipac.caltech.edu/cgi-bin/Gator/nph-scan?mission=irsa&submit=Select&projshort=WISE>



wavelength regimes. The resulting populations from each reduction step can be found in Table 1.

Population	OGLE	QSO	AGN	SF	SB	LRGs	YSOs	Locus	Total
Original	46,262	122,550	19,184	232,845	67,128	105,631	290	25,254	<b>619,267</b>
WISE match	43,209	6,902	3,098	36,539	10,359	75,543	274	25,254	<b>201,178</b>
W1-3, $K_s$ saturation limit	43,201	6,900	3,098	36,538	10,358	75,527	214	25,156	<b>200,992</b>
W1-2 faint limit	43,200	6,891	3,098	36,537	10,358	75,527	214	24,382	<b>200,207</b>
W1-3 faint limit	19,358	6,728	3,005	35,678	10,105	1,184	214	3,154	<b>79,426</b>
W1-3, $K_s$ faint limit	19,358	5,283	2,878	34,299	9,676	1,167	213	3,070	<b>75,944</b>
W1-3 SNR > 3	18,995	5,279	2,876	34,285	9,673	1,079	213	3,056	<b>75,456</b>
cc_flag = 0	9,239	5,029	2,741	32,805	9,219	1,038	184	3,056	<b>63,308</b>

Table 1: Sample populations with respect to each reduction step. Please see section 2.6 for the appropriate saturation limits, faint limits, and WISE matching radii.

### 3. Object Selection Criteria

In producing our candidate sample, we must consider our likely physical sources of contamination, and how removing those sources reduces the completeness of our criteria. In Section 3.1 we consider sample completeness and contamination, and use the sample sets from Section 2.6 to draw simple criteria in WISE-2MASS color-color space. YSOs present a special case of IR contaminants, as they are fairly well embedded in the same regions as AGB stars. We consider the special case of YSOs in Section 3.2, developing finer criteria to remove these objects while still preserving as much of the AGB sample as possible.

#### 3.1. Completeness and Contamination of Initial Samples

Sample completeness  $\eta$  is defined as

$$\eta = \frac{N - n_{\text{missed}}}{N}$$

where  $N$  is the total number of objects in the sample, and  $n_{\text{missed}}$  is the number of objects outside of the applied boundaries. Ivezić et al. (2013) defines sample contamination as

$$\epsilon = \frac{n_{\text{spurious}}}{n_{\text{selected}}}.$$

where  $n_{\text{spurious}}$  is the number of spurious sources and  $n_{\text{selected}} = N + n_{\text{spurious}}$ . Our goal is to get the lowest AGB sample ( $\leq 2\%$  contamination) while still retaining a large number of AGB stars.

The difficulty with determining contamination is that none of the contaminant sample, save for the locus stars, falls within the region occupied by our AGB sample: the LMC. However, knowing

that there is essentially a uniform distribution of extragalactic sources on the sky [a citation would be great], we solve for the number density of objects in the 10,417 sq. deg. DR7 footprint. We then scale these number densities up by the  $\sim 76.5 \text{ deg}^2$  area occupied by the LMC. This should provide a reasonable estimate for the number of sources that we would find within the region of the LMC, and by consequence estimate our final levels of extragalactic contamination in WISE-2MASS color-color space.

We employ the following color criteria to isolate AGB stars from their potential contaminants:

$$(J - K_s) > 1.1 \quad (4)$$

$$-0.1 < (W2 - W3) < 2.5 \quad (5)$$

Figure 5 shows completeness distributions for the OGLE-2MASS-WISE AGB sample, and corresponding contamination distributions for each contaminant sample. Table 2 shows the completeness and contamination fractions for each color criterion. We include the lower limit in  $(W2 - W3)$  because, although there’s a higher penalty on completeness than reduction in contamination, we want to exclude the spike of locus stars with  $(W2 - W3) < -0.1$ .

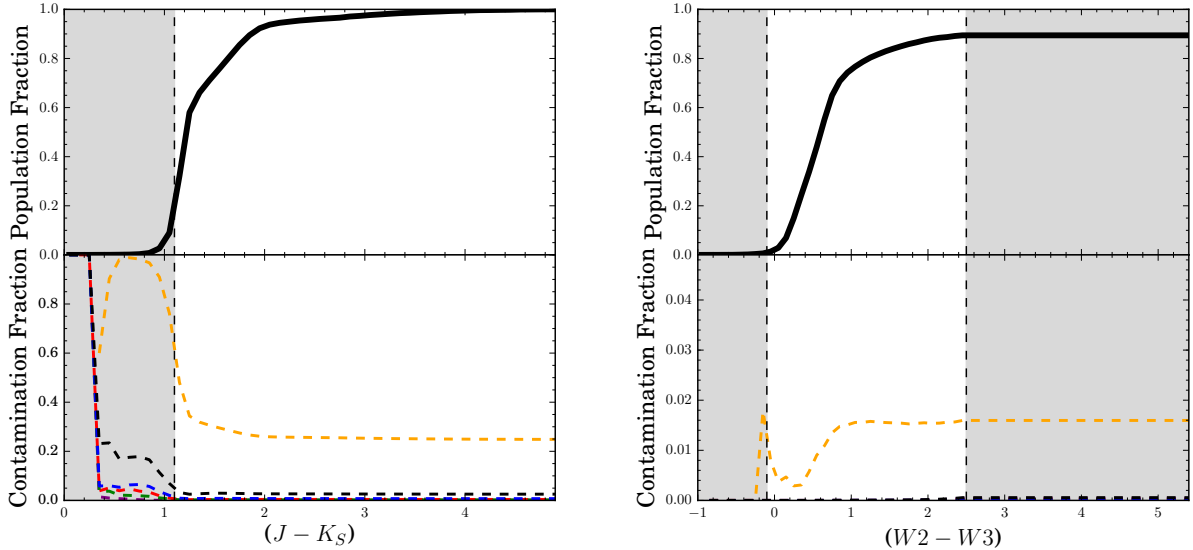


Fig. 5.— *Left*: Cumulative completeness and contamination distributions before  $(J - K_s)$  color cut. *Right*: Cumulative completeness and contamination after  $(J - K_s)$  cut and before  $(W2 - W3)$  cuts. Colors are the same as Figure 3. Thick black line in top panels is OGLE-2MASS-WISE AGB completeness as a function of color. Bin width for both panels is 0.1 dex.

Figure 6 shows the distribution of recovered AGB stars on the sky as well as in color-color space. We reserve an accounting of YSOs for the next section, as there is significant overlap between YSOs and AGBs, and they are not evenly distributed across the sky.

Critiera	QSO	AGN	LRG	SF	SB	Locus	<b>AGB Completeness</b>
$(J - K_s) > 1.1$	0.34%	0.18 %	0.09%	0.34%	0.60%	4.48%	90.97%
$(W2 - W3) < 2.2$	0.03%	0%	0.04%	0.03%	0.02%	1.60%	89.43%
$(W2 - W3) > -0.1$	0.03%	0%	0.04%	0.03%	0.02%	1.59%	88.83%

Table 2: Sample contamination and completeness (*bold*) with respect to each successive cut on WISE-2MASS color.

### 3.2. Accounting for YSOs

YSOs often directly overlap with AGB stars in WISE color-color space, so we treat these objects separately from our extragalactic contaminants. [Rebull et al. \(2011\)](#) produced a catalog of YSOs in the Taurus Molecular Cloud to bring the total number of YSOs in that region up to 290. We use these and the AGB candidate criteria from Section 3.1 to further refine our criteria and increase the purity of our sample.

Figure 7 shows these 290 YSOs in the field of the Taurus Molecular Cloud, overplotted on WISE objects in that field. As shown in Table 1, after photometric and quality cuts we are left with 184 YSOs, and only 74 after applying equations 4 & 5. In contrast, applying equations 4 & 5 as well as photometric criteria from Section 2.6 to the WISE field in the Taurus Molecular Cloud yields 6,995 AGB candidates. Figure 8 shows the degree of entanglement in color-color space for YSOs and AGB candidates. We note, however, that because these are galactic AGB candidates, and the Milky Way is deficient in C-rich AGB stars, Figure 8 misses the degree to which YSOs contaminate the C-rich sequence of AGB stars. To clarify this, we compare Taurus YSOs to AGB stars from the LMC (Figure 9). Based on their positions in color-color space, we add three more constraints to remove YSOs from our AGB candidate sample:

$$(W1 - W2) < 0.75(W2 - W3) - 0.33 \quad \text{for } (W2 - W3) > 1.075 \quad (6)$$

$$(W1 - W2) > -(W2 - W3) + 1.5 \quad \text{for } (W2 - W3) > 1.075 \quad (7)$$

$$(W1 - W2) > 0.2 \quad \text{for } (W2 - W3) > 1.3 \quad (8)$$

Collectively, these criteria preserve the C-rich AGB sequence, retain a relatively high completeness fraction for the LMC objects (82.72%), and reduce the contamination in the Taurus Molecular Cloud due to YSOs from 1.91% to 0.4%.

## 4. AGB Candidate Distribution

Put words here

## 5. Conclusions

Put words here

## REFERENCES

- Bahcall, J. N., & Soneira, R. M. 1980, *Ap. J. Suppl.*, 44, 73
- Belokurov, V., et al. 2006, *Ap. J. (Letters)*, 642, L137
- Benjamin, R. A., et al. 2003, *Pub. A.S.P.*, 115, 953
- Berry, M., et al. 2012, *Ap. J.*, 757, 166
- Blanton, M. R., et al. 2005, *A. J.*, 129, 2562
- Bond, N. A., et al. 2010, *Ap. J.*, 716, 1
- Boyer, M. L., et al. 2011, *A. J.*, 142, 103
- Churchwell, E., et al. 2009, *Pub. A.S.P.*, 121, 213
- Cutri, R. M., et al. 2012, Explanatory Supplement to the WISE All-Sky Data Release Products, Tech. rep.
- . 2013, Explanatory Supplement to the AllWISE Data Release Products, Tech. rep.
- Davenport, J. R. A., et al. 2014, *M.N.R.A.S.*, 440, 3430
- Eisenstein, D. J., et al. 2001, *A. J.*, 122, 2267
- Gilmore, G., Wyse, R. F. G., & Kuijken, K. 1989, *Ann. Rev. Astr. Ap.*, 27, 555
- Grillmair, C. J. 2006, *Ap. J. (Letters)*, 651, L29
- Habing, H. J., Olmon, F. M., Chester, T., Gillett, F., & Rowan-Robinson, M. 1985, *Astr. Ap.*, 152, L1
- Herwig, F. 2005, *Ann. Rev. Astr. Ap.*, 43, 435
- Iben, Jr., I., & Renzini, A. 1983, *Ann. Rev. Astr. Ap.*, 21, 271
- Ivezić, Ž., Connolly, A., VanderPlas, J., & Gray, A. 2013, Statistics, Data Mining, and Machine Learning in Astronomy
- Ivezić, Ž., et al. 2000, *A. J.*, 120, 963
- . 2008, *Ap. J.*, 684, 287

- Jackson, T., Ivezić, Ž., & Knapp, G. R. 2002, *M.N.R.A.S.*, 337, 749
- Jurić, M., et al. 2008, *Ap. J.*, 673, 864
- Kazin, E. A., et al. 2010, *Ap. J.*, 710, 1444
- Knauer, T. G., Ivezić, Ž., & Knapp, G. R. 2001, *Ap. J.*, 552, 787
- Majewski, S. R. 1993, *Ann. Rev. Astr. Ap.*, 31, 575
- Majewski, S. R., Skrutskie, M. F., Weinberg, M. D., & Ostheimer, J. C. 2003, *Ap. J.*, 599, 1082
- Matsuura, M., et al. 2005, *Astr. Ap.*, 434, 691
- Newberg, H. J., et al. 2002, *Ap. J.*, 569, 245
- Olofsson, H., González Delgado, D., Kerschbaum, F., & Schöier, F. L. 2002, *Astr. Ap.*, 391, 1053
- Rebull, L. M., et al. 2011, *Ap. J. Suppl.*, 196, 4
- Saito, R. K., et al. 2012, *Astr. Ap.*, 537, A107
- Sesar, B., et al. 2010, *Ap. J.*, 708, 717
- Skrutskie, M. F., et al. 2006, *A. J.*, 131, 1163
- Soszynski, I., et al. 2007, *Acta Astronomica*, 57, 201
- Soszynski, I., Udalski, A., Kubiak, M., Szymanski, M., Pietrzynski, G., Zebrun, K., Szewczyk, O., & Wyrzykowski, L. 2004, *Acta Astronomica*, 54, 129
- Soszynski, I., et al. 2005, *Acta Astronomica*, 55, 331
- Soszyński, I., et al. 2009, *Acta Astronomica*, 59, 239
- . 2011, *Acta Astronomica*, 61, 217
- Udalski, A., Szymanski, M. K., Soszynski, I., & Poleski, R. 2008, *Acta Astronomica*, 58, 69
- Vivas, A. K., & Zinn, R. 2006, *A. J.*, 132, 714
- Vivas, A. K., et al. 2001, *Ap. J. (Letters)*, 554, L33
- Wood, P. R., et al. 1999, in IAU Symposium, Vol. 191, Asymptotic Giant Branch Stars, ed. T. Le Bertre, A. Lebre, & C. Waelkens, 151
- Wright, E. L., et al. 2010, *A. J.*, 140, 1868
- Yanny, B., et al. 2000, *Ap. J.*, 540, 825

York, D. G., et al. 2000, *A. J.*, 120, 1579

Zebrun, K., Soszynski, I., & Wozniak, P. R. 2001, *Acta Astronomica*, 51, 303

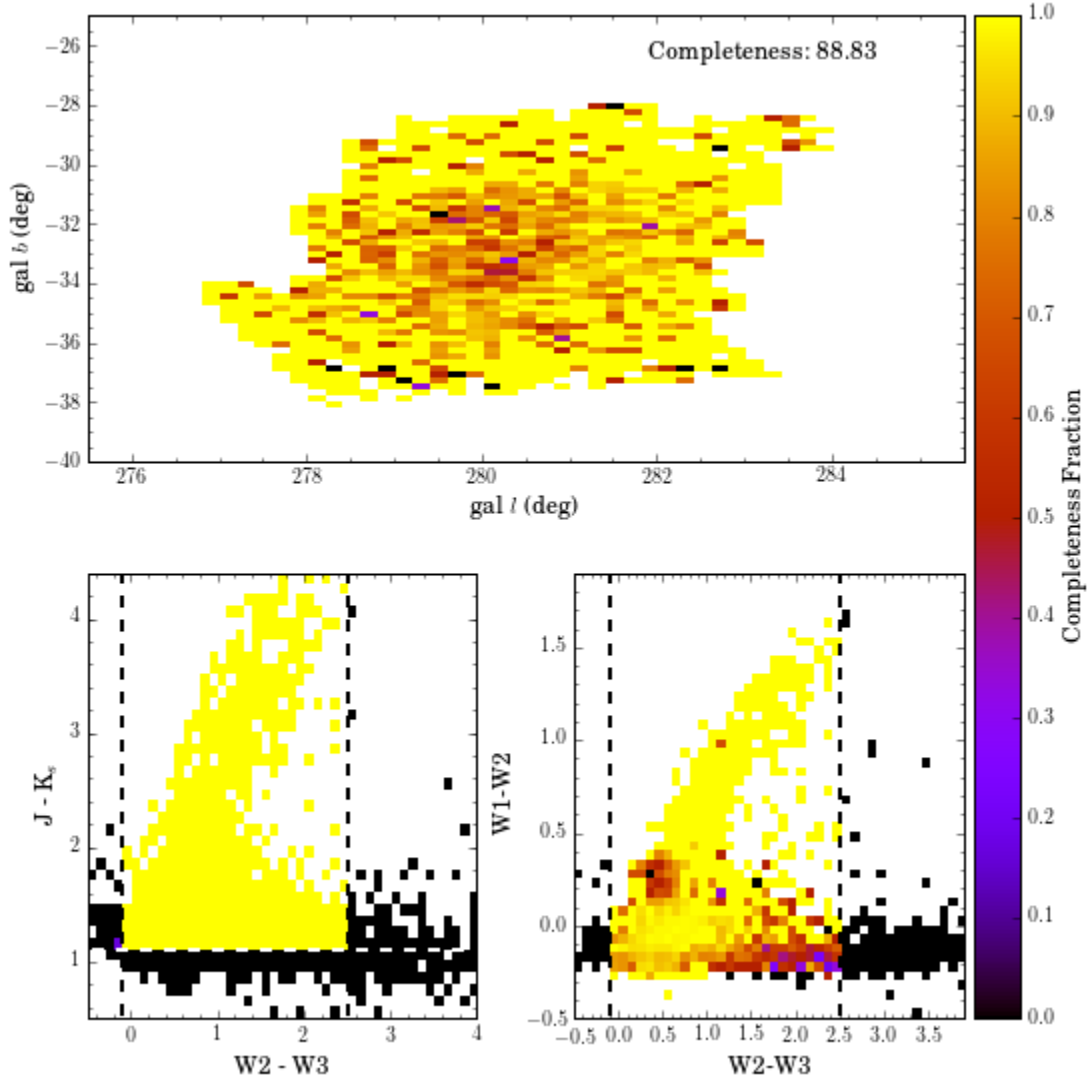


Fig. 6.— Map of completeness fractions for AGB stars in the LMC



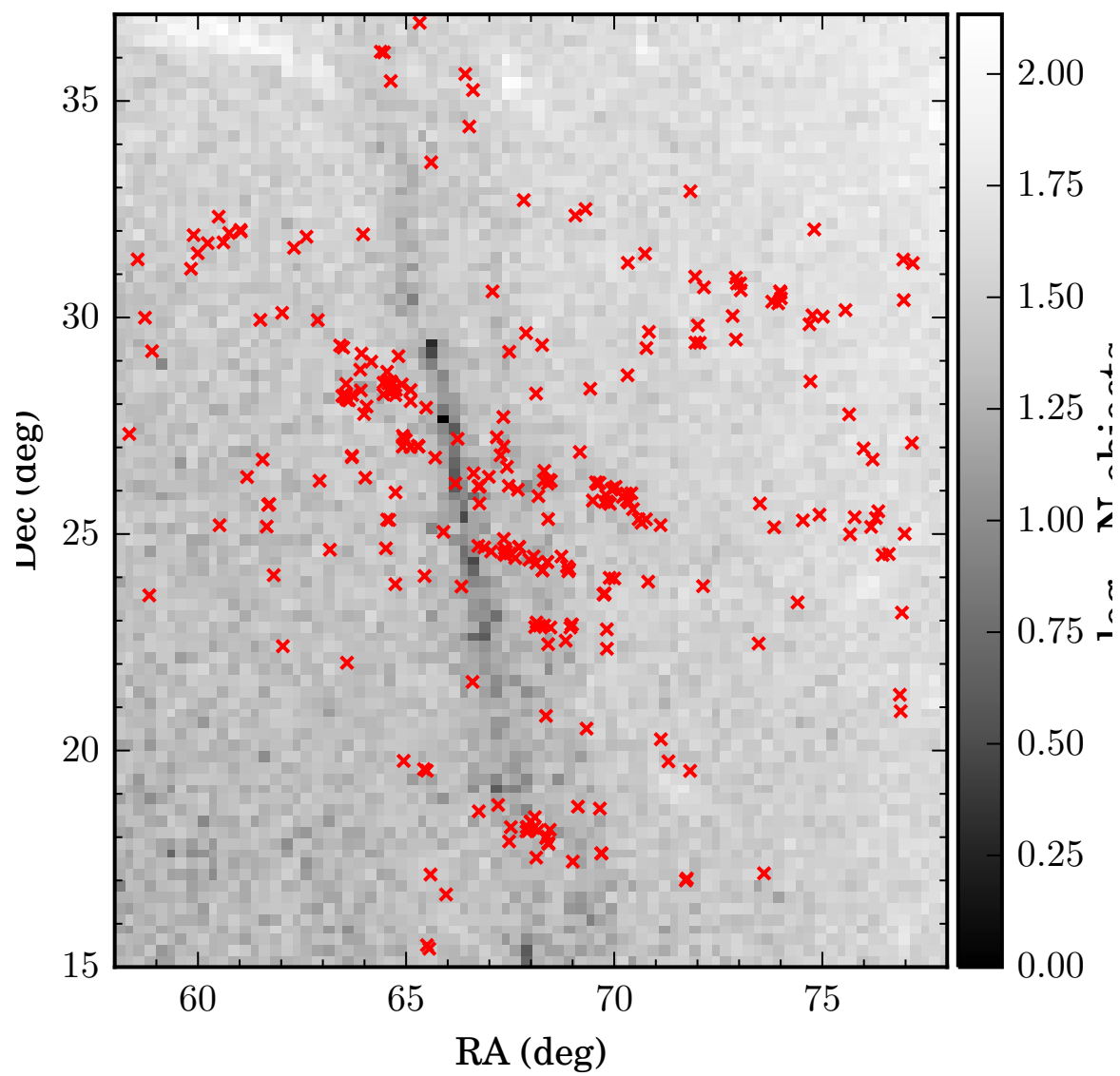


Fig. 7.— YSOs (*red x*) in the Taurus Molecular Cloud ([Rebull et al. 2011](#)).

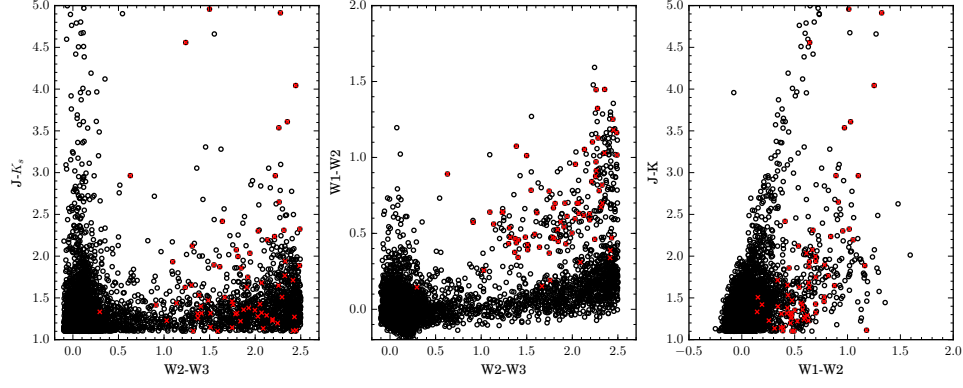


Fig. 8.— YSOs (*red x*) and AGB candidates (*black o*) in the Taurus Molecular Cloud.

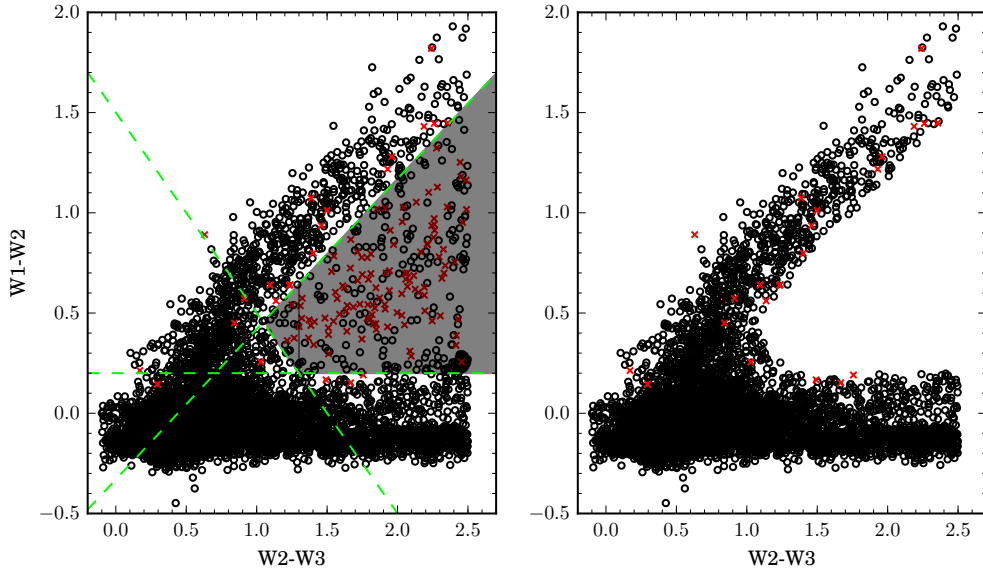


Fig. 9.— YSOs (*red x*) and AGB candidates (*black o*) in the Taurus Molecular Cloud.